

Beta-adrenergic receptor stimulation limits the cellular proarrhythmic effects of chloroquine and azithromycin

Henry Sutanto, MD, MSc¹ and Jordi Heijman, PhD¹

¹Department of Cardiology, CARIM School for Cardiovascular Diseases, Maastricht University, Maastricht, The Netherlands.

Short running title: Sutanto – chloroquine and azithromycin in COVID-19

Word count: 2486 (excluding abstract, methods, references and figure legends)

Conflict of Interest: None

Corresponding Author:

Jordi Heijman, PhD

Dept. of Cardiology, CARIM School for Cardiovascular Diseases, Maastricht University

PO Box 616, 6200 MD, Maastricht, The Netherlands

E-Mail: jordi.heijman@maastrichtuniversity.nl

Abstract

Background and purpose: The antimalarial drug chloroquine and antimicrobial drug azithromycin have received significant attention during the current COVID-19 pandemic. Both drugs can alter cardiac electrophysiology and have been associated with drug-induced arrhythmias. Meanwhile, sympathetic activation is commonly observed during systemic inflammation and oxidative stress (e.g., in SARS-CoV-2 infection), and may influence the electrophysiological effects of chloroquine and azithromycin. Here, we investigated the effect of beta-adrenergic stimulation on proarrhythmic properties of chloroquine and azithromycin using a detailed *in silico* model of ventricular electrophysiology.

Experimental approach: Concentration-dependent chloroquine and azithromycin-induced alterations in ion-channel function were incorporated into the Heijman canine ventricular cardiomyocyte model. Single and combined drug effects on action-potential (AP) properties were analyzed using a population of 592 models accommodating inter-individual variability. Sympathetic stimulation was simulated by an increase in pacing rate and experimentally validated isoproterenol-induced changes in ion-channel function.

Key results: At 1 Hz pacing, therapeutic doses of chloroquine and azithromycin (5 and 20 μM , respectively) individually prolonged AP duration (APD) by 33% and 13%. Their combination produced synergistic APD prolongation (+161%) with incidence of proarrhythmic early afterdepolarizations in 53.5% of models. Increasing the pacing frequency to 2 Hz shortened APD and together with 1 μM isoproterenol corrected the drug-induced APD prolongation. No afterdepolarizations occurred following increased rate and simulated application of 0.1-1 μM isoproterenol.

Conclusion and Implications: Sympathetic stimulation limits chloroquine- and azithromycin-induced proarrhythmia by reducing their APD-prolonging effect, suggesting the importance of heart rate and autonomic status monitoring in particular conditions (e.g., COVID-19).

Keywords: arrhythmia; computational modeling; COVID-19; chloroquine; azithromycin; beta-adrenergic; electrophysiology.

Abbreviations

ACE2	Angiotensin converting enzyme type 2
AP	Action potential
APD	Action potential duration
AZM	Azithromycin
Ca ²⁺	Calcium
CaMKII	Ca ²⁺ /calmodulin-dependent protein kinase II
CoV	Coronavirus
COVID-19	Coronavirus disease 2019
CQ	Chloroquine
EAD	Early afterdepolarization
IQR	Interquartile range
ISO	Isoproterenol
K ⁺	Potassium
PKC	Protein kinase-C
RF	Repolarization failure
RMP	Resting membrane potential
ROS	Reactive oxygen species
SARS	Severe acute respiratory syndrome

1. Introduction

Six-months after its first identification in Wuhan, China in December 2019, Severe Acute Respiratory Syndrome-associated Coronavirus type-2 (SARS-CoV-2) infection (i.e., Coronavirus Disease 2019 / COVID-19) has contributed to more than 500,000 deaths worldwide and has been declared a pandemic with significant global socioeconomic impact (1). At the moment, the exact pathophysiology of the disease remains unclear and no definitive therapy is available. Several drugs are considered effective in preclinical studies and are currently being tested against SARS-CoV-2 in the clinic (e.g., the antivirals lopinavir, ritonavir, and remdesivir; the antimicrobial azithromycin; the antimalarial drugs chloroquine and hydroxychloroquine, and more recently antiparasitic ivermectin) (2-4). Of those, chloroquine (CQ) and azithromycin (AZM) have gained significant attention due to their high accessibility and low cost. Nonetheless, their effectivity against COVID-19 has not been confirmed by any large clinical trial and their use is controversial. Some studies reported the benefit of those drugs (5-7), while others reported no effect (8, 9). This controversy is further complicated by the retraction of papers demonstrating the absence of benefit of these drugs in COVID-19 (8) and the termination of their emergency use by the United States Food and Drug Administration (FDA) due to their potential proarrhythmic effects (10).

CQ is a widely-used antimalarial drug that inhibits multiple cardiac ion-channels (11). It has been suggested to prevent the viral entry, transport and post-entry events in COVID-19, although the exact mechanisms remain unknown (12). Meanwhile, AZM is a broad-spectrum macrolide antibiotic that is believed to potentiate the effect of CQ, reducing the replication capabilities of SARS-CoV-2 (12). Similar to CQ, AZM also inhibits multiple cardiac ion-channels in a dose-dependent manner (11). Therefore, the administration of CQ and AZM, alone or in combination, can prolong the ventricular cardiomyocyte action potential duration (APD) and thereby the QT interval on the electrocardiogram. Excessive QT-interval prolongation has been implicated in drug-induced malignant arrhythmias, such as Torsade de Pointes (10, 13, 14), by promoting early afterdepolarizations (EADs) and a heterogeneous repolarization substrate.

Although the cardiac pathophysiology of COVID-19 remains incompletely understood, several aspects point towards increased incidence of cardiac arrhythmias (15). SARS-CoV-2 induces systemic inflammation, leading to cytokine storm (16), which is expected to increase oxidative stress by releasing reactive oxygen species (ROS). Moreover, CQ may itself promote increased oxidative stress (17). Both inflammation and oxidative stress have been associated with increased arrhythmogenic risk, e.g., through activation of Ca^{2+} /calmodulin-dependent protein kinase II (CaMKII) (18, 19) and NLRP3 inflammasome (20), as observed in COVID-19 (21). Moreover, COVID-19 may activate the beta-adrenergic signaling cascade in cardiomyocytes via the stimulation of sympathetic nervous system (16). Altogether, these processes may increase the propensity for cardiac arrhythmias, by altering cardiomyocyte Ca^{2+} -handling and modulating ion-channel properties (**Figure 1**) (22).

Computational modeling has increasingly been used in cardiac safety pharmacology to predict the proarrhythmic effect of novel compounds (23-25). To the best of our knowledge, previous analyses of the potential proarrhythmic effects of CQ and AZM have not considered the role of beta-adrenergic receptor stimulation. Therefore, this study aimed to assess the potential cellular proarrhythmic effects of CQ and AZM in both the absence and presence of beta-adrenergic receptor stimulation using a population of detailed *in silico* models of ventricular electrophysiology.

2. Methods

Concentration-dependent CQ and AZM-induced alterations in 7 ion-channels (rapid delayed-rectifier K^+ (I_{Kr}), fast Na^+ (I_{Na}), late Na^+ (I_{NaL}), transient-outward K^+ (I_{to}), inward-rectifier K^+ (I_{K1}) and slow delayed-rectifier K^+ current (I_{Ks})) (11) (**Figure 2**) were incorporated into the Heijman canine ventricular cardiomyocyte model (26) with beta-adrenergic receptor signaling. A cellular concentration within the therapeutic range of CQ and AZM was selected (5 and 20 μM , respectively (27, 28)) and cellular simulations were performed in Myokit (29). The effects of the drugs alone and in combination (assuming independent drug-binding sites) on action potential (AP) properties were assessed. Sympathetic stimulation was simulated by an increase in pacing rate and experimentally validated isoproterenol-induced changes in ion-channel function (26, 30). All results are

presented during steady-state pacing at the indicated pacing frequencies (after 1000 beats of prepacing). To evaluate the robustness of our findings and assess potential consequences of intra- and inter-subject variability on the electrophysiological effect of CQ and AZM, the maximum conductance of 9 major ionic currents (I_{Na} , I_{NaL} , $I_{Ca,L}$, I_{Kr} , I_{Ks} , I_{K1} , I_{to} , I_{NCX} and I_{NaK}) were scaled based on a normal distribution with mean 1.0 and standard deviation 0.2, to create populations of models, as previously described (31). In brief, 1000 variants of the model were created and the variants displaying “non-physiological” AP properties (defined as APD_{90} or RMP outside the range of 3 standard deviations of experimental APD_{90} and RMP from (32)) were excluded. In total, 592 out of 1000 models were included. The non-normally distributed data are presented as median and inter-quartile ranges (IQR). The model code is available at www.github.com/jordiheijman.

3. Results

During 1 Hz pacing, application of 5 μ M CQ in the Heijman canine ventricular epicardial myocyte model prolonged APD by 70 ms (+33%), while 20 μ M AZM prolonged APD by 27 ms (+13%). The combination of both drugs showed a synergistic effect with an APD prolongation of 339 ms (+161%) and the occurrence of an EAD, as shown in **Figure 3A, upper panels**. Subsequently, the contributions of beta-adrenergic-dependent signaling cascades were assessed in two ways: by increasing the pacing frequency and through the simulated application of a maximal concentration of the beta-adrenergic receptor agonist isoproterenol (ISO; 1 μ M) in combination with the escalation of pacing rate. Increasing the pacing rate from 1 to 2 Hz reduced the APD in all groups, with APD reduction of 14 ms (-7%) in the non-treated, 28 ms (-10%) in the CQ, 21 ms (-9%) in the AZM and 261 ms (-47%) in the combined groups. The previously observed EAD in the combined group was not observed following the increase in pacing rate (**Figure 3A, middle panels**). The combination of simulated ISO application and increased pacing rate further reduced APD, with APD reduction of 40 ms (-19%) in the non-treated, 84 ms (-30%) in the CQ, 53 ms (-22%) in the AZM and 341 ms (-62%) in the combined groups compared to APD during 1 Hz pacing (**Figure 3A, lower panels**). Consistently, increasing the pacing rate up to 4 Hz further reduced APD and lowering the pacing rate from 1 to

0.25 Hz prolonged the APD and resulted in EADs in the combined CQ+AZM group (**Figure 3B, left and middle panels**). Furthermore, at pacing rates >1 Hz, AZM slightly hyperpolarized the RMP, which was opposed by the RMP-depolarizing effect of beta-adrenergic activation, while CQ with or without ISO consistently showed a slight depolarization of RMP, likely due to its inhibition of I_{K1} (**Figure 2**). The RMP modulating effect is attenuated at low pacing rates (**Figure 3B, right panel**).

The beta-adrenergic-induced modification of 8 ionic currents (I_{NaL} , $I_{Ca,L}$, I_{to} , I_{Kr} , I_{Ks} , I_{K1} , I_{NCX} and I_{NaK}) can be seen in **Figure 4**, highlighting the significantly increased I_{Ks} during beta-adrenergic stimulation. Indeed, ISO-induced phosphorylation of I_{Ks} and $I_{Ca,L}$ contributed to the previously observed APD reduction in the model, as previously documented (26) and preventing such phosphorylation resulted in repolarization failure (RF) in the CQ+AZM group in the presence of simulated beta-adrenergic stimulation (**Figure 5**).

Next, a population-based study was conducted to accommodate intra- and interindividual variability. A population of 1000 models was created by varying 9 ionic currents conductance as described in the **Methods**. After the exclusion of models with non-physiological baseline APs, 592 models were included in the population (**Figure 6A, upper panels, blue lines** and **Figure 6G**). To simulate inter-individual differences in beta-adrenergic activation, a random concentration of ISO from 0.1 to 1 μ M was assigned to each model (**Figure 6H**). Consistent with the default model without variability, at 1 Hz pacing, CQ (5 μ M) prolonged the APD by a median 73.3 ms (IQR 67.5-82.3). Similarly, AZM 20 μ M prolonged the APD by a median 28.7 ms (IQR 25.5-36.3) and the combination of CQ and AZM prolonged the APD with median 146.5 ms (IQR 92.1-334.7). During 2 Hz pacing, CQ, AZM and CQ+AZM prolonged the APD with median 59 ms (IQR 56.7-62), 22.7 ms (IQR 20.8-25.5), and 95.2 ms (IQR 84.2-109.3), respectively. Finally, following the addition of ISO, the APD prolongation was further reduced with median prolongation of 26.5 ms (IQR 25.3-27.9) in CQ, 13.5 ms (IQR 13.1-14.2) in AZM and 37.6 ms (IQR 35.7-40.7) in combined groups (**Figure 6A-E**).

Finally, the incidence of EADs and RF in the population of models was calculated (**Figure 6F**). During 1 Hz pacing, no EAD/RF was documented in the non-treated group, while 6.4% of models in the CQ group, 2.4% of models in the AZM group, and 53.5% of models

in the combined group exhibited EADs/RFs. Following the increase in pacing rate to 2 Hz, the incidence of EAD/RF was reduced to 0.5%, 0.7% and 11.5%, respectively. No EAD/RF was observed in any of the groups following the application of ISO in 2 Hz pacing.

4. Discussion

Here, we investigated the potential proarrhythmic effects of CQ and AZM in the ventricular cardiomyocyte in the absence or presence of beta-adrenergic stimulation using an *in silico* approach. First, our results indicate that CQ and AZM could significantly prolong the APD even within their therapeutic range. Moreover, their combination resulted in a synergistic APD prolongation, leading to the initiation of proarrhythmic EADs. Second, beta-adrenergic stimulation reduced APD prolongation and prevented EAD formation due to the upregulation of I_{Ks} and $I_{Ca,L}$. Finally, our population-based study confirmed the robustness of these findings and showed that beta-adrenergic stimulation completely cancelled the initiation of EADs and RFs in all groups, highlighting a potential important role for beta-adrenergic activity in preventing drug-induced proarrhythmia by CQ and AZM.

4.1 Chloroquine and azithromycin exhibit a synergistic APD-prolonging effect

CQ and AZM block multiple ion channels, including the rapid delayed-rectifier K^+ current (I_{Kr}) (11), which dose-dependently prolongs the APD and increases the propensity for EADs, creating a substrate for cardiac arrhythmias. In the clinic, they are known to prolong the QT interval, increasing the susceptibility for life-threatening arrhythmias, such as Torsade de Pointes. Several studies have also reported the potential proarrhythmic effects of CQ and AZM in COVID-19 patients (10, 13, 14). In this computational study, we confirmed the potentially harmful ventricular APD-prolonging effect of CQ and AZM. However, within the therapeutic range, the incidence of EADs was relatively low (6.4% in CQ group and 2.4% in AZM group). However, the combination of both drugs, as proposed in the treatment of COVID-19, produced a synergistic APD-prolonging effect that further increased the likelihood of EADs, particularly at slow heart rates, suggesting the need for close monitoring of the QT interval during the administration of these drugs in the clinic. In agreement, a previous prospective observational study also showed that the maximum corrected QT interval during treatment was significantly longer in the combination group

compared to the mono therapy group, highlighting the synergy between CQ and AZM (14).

4.2 Beta-adrenergic activation reduces the APD and lowers the cellular proarrhythmic risk of chloroquine and azithromycin

Beta-adrenergic agonists have been used as an antidote against CQ intoxication for a long time (33, 34). Their benefit in the management of CQ-induced arrhythmia has been experimentally demonstrated in anaesthetized rats, showing that the CQ-infused group treated with isoprenaline (a selective beta-adrenergic receptor agonist) displayed longer time to arrhythmias and death (35). Conversely, the administration of propranolol (a beta-adrenergic receptor blocker) potentiated the electrocardiographic effects of CQ, indicating that beta-adrenergic receptor blockade might render the heart more vulnerable to the actions of CQ (36).

In this study, we demonstrated that beta-adrenergic stimulation could be a potential protective factor against CQ- and AZM-induced proarrhythmia by lowering the APD prolongation and preventing the occurrence of afterdepolarizations. Our population-based study showed that the protective effects of beta-adrenergic stimulation are robust, reducing the incidence of EADs and RFs for a large number of virtual genotypes and with a relatively wide range of simulated isoproterenol concentrations. Although extrapolation of these findings to the clinical setting is challenging, they suggest that the concomitant sympathetic stimulation in COVID-19 patients may reduce the likelihood of Torsade de Pointes, or arrhythmogenic death in COVID-19 patients despite the presence of marked QT interval prolongation, in line with observational studies (14).

On the other hand, there has been clear evidence that long-term beta-adrenergic stimulation promotes cardiac remodeling, including hypertrophy, fibrosis and the downregulation of several ion channels via transcriptional and post-translational modifications, potentially creating a substrate for cardiac arrhythmias (22, 37, 38). Therefore, transient activation of the beta-adrenergic response may be beneficial against drug-induced proarrhythmia and beta-blockers might not be appropriate under such circumstances. On the other hand, beta-blockers could be used to reduce the detrimental

effect of long-term beta-adrenergic stimulation or to reduce the complications of COVID-19-induced systemic inflammation in the absence of medications with proarrhythmic behavior.

4.3 Limitations of the study

Here, we performed a computational study using an established canine ventricular cardiomyocyte model with beta-adrenergic signaling (26, 30). Despite similarities between canine and human electrophysiology, future studies integrating all components in a human cardiomyocyte model are warranted. Although EADs are an established proarrhythmic mechanism, extrapolation of the current findings to tissue- or organ-level simulations, taking into account the heterogeneous nature of sympathetic innervation, would be required to confirm the pro- and antiarrhythmic effects identified at the cellular level. These were not performed due to the computational costs associated with the complexity of the cardiomyocyte model and the relatively slow time-course of beta-adrenergic stimulation-induced electrophysiological modulation (requiring long simulations).

In this study, we used the cellular concentrations of CQ and AZM. However, it can be challenging to correlate these cellular concentrations to the clinically relevant doses due to variability in the pharmacokinetics and -dynamics of the drugs, particularly in severely ill patients. Pharmacokinetics/-dynamics models exist and, in the future, could be implemented to obtain a more precise simulation of the electrophysiological consequences of the drugs.

The drug-induced ion-channel modifications incorporated in this study (**Figure 2**) were derived from previous publication using heterologous expression systems (in Chinese hamster ovary / human embryonic kidney cells), which could display different results from human cardiomyocytes (11). Since these data are the only available data to date, we assumed that the relative drug effects are retained across species and cell types.

5. Conclusions

CQ and AZM exhibit a proarrhythmic behavior due to their APD-prolonging effect, with their combination showing a pronounced potentiation of this APD prolongation, posing a

bigger threat for cardiac arrhythmias. Acute activation of the sympathetic nervous system prevents CQ- and AZM-induced proarrhythmia by reducing their APD-prolonging effect, highlighting the importance of preserving the beta-adrenergic response in the presence of such proarrhythmic medications and the potential significance of heart-rate and autonomic-status monitoring in particular conditions such as COVID-19.

Author contributions

HS and JH conceived the study. HS performed the computational simulations. HS and JH performed the data analysis and drafted the manuscript. All authors critically revised the manuscript and approved the final version.

References

1. Nicola M, Alsafi Z, Sohrabi C, Kerwan A, Al-Jabir A, Iosifidis C, et al. The socio-economic implications of the coronavirus pandemic (COVID-19): A review. *Int J Surg* (2020) 78:185-93. doi: 10.1016/j.ijssu.2020.04.018. PubMed PMID: 32305533.
2. Wang Y, Zhang D, Du G, Du R, Zhao J, Jin Y, et al. Remdesivir in adults with severe COVID-19: a randomised, double-blind, placebo-controlled, multicentre trial. *Lancet* (2020) 395(10236):1569-78. doi: 10.1016/S0140-6736(20)31022-9. PubMed PMID: 32423584.
3. Caly L, Druce JD, Catton MG, Jans DA, Wagstaff KM. The FDA-approved drug ivermectin inhibits the replication of SARS-CoV-2 in vitro. *Antiviral Res* (2020) 178:104787. doi: 10.1016/j.antiviral.2020.104787. PubMed PMID: 32251768.
4. Lu CC, Chen MY, Lee WS, Chang YL. Potential therapeutic agents against COVID-19: What we know so far. *J Chin Med Assoc* (2020) 83(6):534-6. doi: 10.1097/JCMA.0000000000000318. PubMed PMID: 32243270.
5. Gao J, Tian Z, Yang X. Breakthrough: Chloroquine phosphate has shown apparent efficacy in treatment of COVID-19 associated pneumonia in clinical studies. *Biosci Trends* (2020) 14(1):72-3. doi: 10.5582/bst.2020.01047. PubMed PMID: 32074550.
6. Colson P, Rolain JM, Lagier JC, Brouqui P, Raoult D. Chloroquine and hydroxychloroquine as available weapons to fight COVID-19. *Int J Antimicrob Agents* (2020) 55(4):105932. doi: 10.1016/j.ijantimicag.2020.105932. PubMed PMID: 32145363.
7. Huang M, Tang T, Pang P, Li M, Ma R, Lu J, et al. Treating COVID-19 with Chloroquine. *J Mol Cell Biol* (2020) 12(4):322-5. doi: 10.1093/jmcb/mjaa014. PubMed PMID: 32236562.
8. Mehra MR, Desai SS, Ruschitzka F, Patel AN. RETRACTED: Hydroxychloroquine or chloroquine with or without a macrolide for treatment of COVID-19: a multinational registry analysis. *Lancet* (2020). doi: 10.1016/S0140-6736(20)31180-6. PubMed PMID: 32450107.
9. Molina JM, Delaugerre C, Le Goff J, Mela-Lima B, Ponscarne D, Goldwirt L, et al. No evidence of rapid antiviral clearance or clinical benefit with the combination of hydroxychloroquine and azithromycin in patients with severe COVID-19 infection. *Med Mal Infect* (2020) 50(4):384. doi: 10.1016/j.medmal.2020.03.006. PubMed PMID: 32240719.
10. Uzelac I, Iravanian S, Ashikaga H, Bhatia NK, Herndon C, Kaboudian A, et al. Fatal arrhythmias: Another reason why doctors remain cautious about chloroquine/hydroxychloroquine for treating COVID-19. *Heart Rhythm* (2020). doi: 10.1016/j.hrthm.2020.05.030. PubMed PMID: 32479900.
11. Crumb WJ, Jr., Vicente J, Johannesen L, Strauss DG. An evaluation of 30 clinical drugs against the comprehensive in vitro proarrhythmia assay (CiPA) proposed ion channel panel. *J Pharmacol Toxicol Methods* (2016) 81:251-62. doi: 10.1016/j.vascn.2016.03.009. PubMed PMID: 27060526.
12. Singh AK, Singh A, Shaikh A, Singh R, Misra A. Chloroquine and hydroxychloroquine in the treatment of COVID-19 with or without diabetes: A systematic search and a narrative review with a special reference to India and other developing countries. *Diabetes Metab Syndr* (2020) 14(3):241-6. doi: 10.1016/j.dsx.2020.03.011. PubMed PMID: 32247211.

13. van den Broek MPH, Mohlmann JE, Abeln BGS, Liebregts M, van Dijk VF, van de Garde EMW. Chloroquine-induced QTc prolongation in COVID-19 patients. *Neth Heart J* (2020). doi: 10.1007/s12471-020-01429-7. PubMed PMID: 32350818.
14. Saleh M, Gabriels J, Chang D, Soo Kim B, Mansoor A, Mahmood E, et al. Effect of Chloroquine, Hydroxychloroquine, and Azithromycin on the Corrected QT Interval in Patients With SARS-CoV-2 Infection. *Circ Arrhythm Electrophysiol* (2020) 13(6):e008662. doi: 10.1161/CIRCEP.120.008662. PubMed PMID: 32347743.
15. Bhatla A, Mayer MM, Adusumalli S, Hyman MC, Oh E, Tierney A, et al. COVID-19 and Cardiac Arrhythmias. *Heart Rhythm* (2020). doi: 10.1016/j.hrthm.2020.06.016. PubMed PMID: 32585191.
16. Lazzerini PE, Boutjdir M, Capecchi PL. COVID-19, Arrhythmic Risk and Inflammation: Mind the Gap! *Circulation* (2020). doi: 10.1161/CIRCULATIONAHA.120.047293. PubMed PMID: 32286863.
17. Murphy KR, Baggett B, Cooper LL, Lu Y, J OU, Sedivy JM, et al. Enhancing Autophagy Diminishes Aberrant Ca²⁺ Homeostasis and Arrhythmogenesis in Aging Rabbit Hearts. *Front Physiol* (2019) 10:1277. doi: 10.3389/fphys.2019.01277. PubMed PMID: 31636573.
18. Wang Q, Quick AP, Cao S, Reynolds J, Chiang DY, Beavers D, et al. Oxidized CaMKII (Ca²⁺/Calmodulin-Dependent Protein Kinase II) Is Essential for Ventricular Arrhythmia in a Mouse Model of Duchenne Muscular Dystrophy. *Circ Arrhythm Electrophysiol* (2018) 11(4):e005682. doi: 10.1161/CIRCEP.117.005682. PubMed PMID: 29654126.
19. Yoo S, Aistrup G, Shiferaw Y, Ng J, Mohler PJ, Hund TJ, et al. Oxidative stress creates a unique, CaMKII-mediated substrate for atrial fibrillation in heart failure. *JCI Insight* (2018) 3(21). doi: 10.1172/jci.insight.120728. PubMed PMID: 30385719.
20. Yao C, Veleva T, Scott L, Jr., Cao S, Li L, Chen G, et al. Enhanced Cardiomyocyte NLRP3 Inflammasome Signaling Promotes Atrial Fibrillation. *Circulation* (2018) 138(20):2227-42. doi: 10.1161/CIRCULATIONAHA.118.035202. PubMed PMID: 29802206.
21. Shah A. Novel Coronavirus-Induced NLRP3 Inflammasome Activation: A Potential Drug Target in the Treatment of COVID-19. *Front Immunol* (2020) 11:1021. doi: 10.3389/fimmu.2020.01021. PubMed PMID: 32574259.
22. Sutanto H, Lyon A, Lumens J, Schotten U, Dobrev D, Heijman J. Cardiomyocyte calcium handling in health and disease: Insights from in vitro and in silico studies. *Prog Biophys Mol Biol* (2020). doi: 10.1016/j.pbiomolbio.2020.02.008. PubMed PMID: 32188566.
23. Li Z, Mirams GR, Yoshinaga T, Ridder BJ, Han X, Chen JE, et al. General Principles for the Validation of Proarrhythmia Risk Prediction Models: An Extension of the CiPA In Silico Strategy. *Clin Pharmacol Ther* (2020) 107(1):102-11. doi: 10.1002/cpt.1647. PubMed PMID: 31709525.
24. Ridder BJ, Leishman DJ, Bridgland-Taylor M, Samieegohar M, Han X, Wu WW, et al. A systematic strategy for estimating hERG block potency and its implications in a new cardiac safety paradigm. *Toxicol Appl Pharmacol* (2020) 394:114961. doi: 10.1016/j.taap.2020.114961. PubMed PMID: 32209365.

25. Qu Y, Vargas H, Rodriguez B, Zhou X, Passini E, Liu Y, et al. Pro-arrhythmic risk assessment with a population model of human ventricular myocyte action potentials. *J Pharmacol Toxicol Methods* (2019) 99:106595. doi: 10.1016/j.vascn.2019.05.105. PubMed PMID: 31962987.
26. Heijman J, Volders PG, Westra RL, Rudy Y. Local control of beta-adrenergic stimulation: Effects on ventricular myocyte electrophysiology and Ca^{2+} -transient. *J Mol Cell Cardiol* (2011) 50(5):863-71. doi: 10.1016/j.yjmcc.2011.02.007. PubMed PMID: 21345340.
27. Wang M, Cao R, Zhang L, Yang X, Liu J, Xu M, et al. Remdesivir and chloroquine effectively inhibit the recently emerged novel coronavirus (2019-nCoV) in vitro. *Cell Res* (2020) 30(3):269-71. doi: 10.1038/s41422-020-0282-0. PubMed PMID: 32020029.
28. Gielen V, Johnston SL, Edwards MR. Azithromycin induces anti-viral responses in bronchial epithelial cells. *Eur Respir J* (2010) 36(3):646-54. doi: 10.1183/09031936.00095809. PubMed PMID: 20150207.
29. Clerx M, Collins P, de Lange E, Volders PG. Myokit: A simple interface to cardiac cellular electrophysiology. *Prog Biophys Mol Biol* (2016) 120(1-3):100-14. doi: 10.1016/j.pbiomolbio.2015.12.008. PubMed PMID: 26721671.
30. Tomek J, Rodriguez B, Bub G, Heijman J. beta-Adrenergic receptor stimulation inhibits proarrhythmic alternans in postinfarction border zone cardiomyocytes: a computational analysis. *Am J Physiol Heart Circ Physiol* (2017) 313(2):H338-H53. doi: 10.1152/ajpheart.00094.2017. PubMed PMID: 28550171.
31. Sobie EA. Parameter sensitivity analysis in electrophysiological models using multivariable regression. *Biophys J* (2009) 96(4):1264-74. doi: 10.1016/j.bpj.2008.10.056. PubMed PMID: 19217846.
32. Anyukhovskiy EP, Sosunov EA, Rosen MR. Regional differences in electrophysiological properties of epicardium, midmyocardium, and endocardium. In vitro and in vivo correlations. *Circulation* (1996) 94(8):1981-8. doi: 10.1161/01.cir.94.8.1981. PubMed PMID: 8873677.
33. Don Michael TA, Aiwazzadeh S. The effects of acute chloroquine poisoning with special reference to the heart. *Am Heart J* (1970) 79(6):831-42. doi: 10.1016/0002-8703(70)90371-6. PubMed PMID: 5419357.
34. Jaeger A, Raguin O, Liegeon MN. Acute poisoning by class I anti-arrhythmia agents and by chloroquine. *Rev Prat* (1997) 47(7):748-53. PubMed PMID: 9183952.
35. Buckley NA, Smith AJ, Dosen P, O'Connell DL. Effects of catecholamines and diazepam in chloroquine poisoning in barbiturate anaesthetised rats. *Hum Exp Toxicol* (1996) 15(11):909-14. doi: 10.1177/096032719601501108. PubMed PMID: 8938487.
36. Sofola OA. The effects of chloroquine on the electrocardiogram and heart rate in anaesthetized dogs. *Clin Physiol* (1983) 3(1):75-82. doi: 10.1111/j.1475-097x.1983.tb00701.x. PubMed PMID: 6682027.
37. Scheuer J. Catecholamines in cardiac hypertrophy. *Am J Cardiol* (1999) 83(12A):70H-4H. doi: 10.1016/s0002-9149(99)00264-7. PubMed PMID: 10750591.

38. Dang S, Zhang ZY, Li KL, Zheng J, Qian LL, Liu XY, et al. Blockade of beta-adrenergic signaling suppresses inflammasome and alleviates cardiac fibrosis. *Ann Transl Med* (2020) 8(4):127. doi: 10.21037/atm.2020.02.31. PubMed PMID: 32175420.

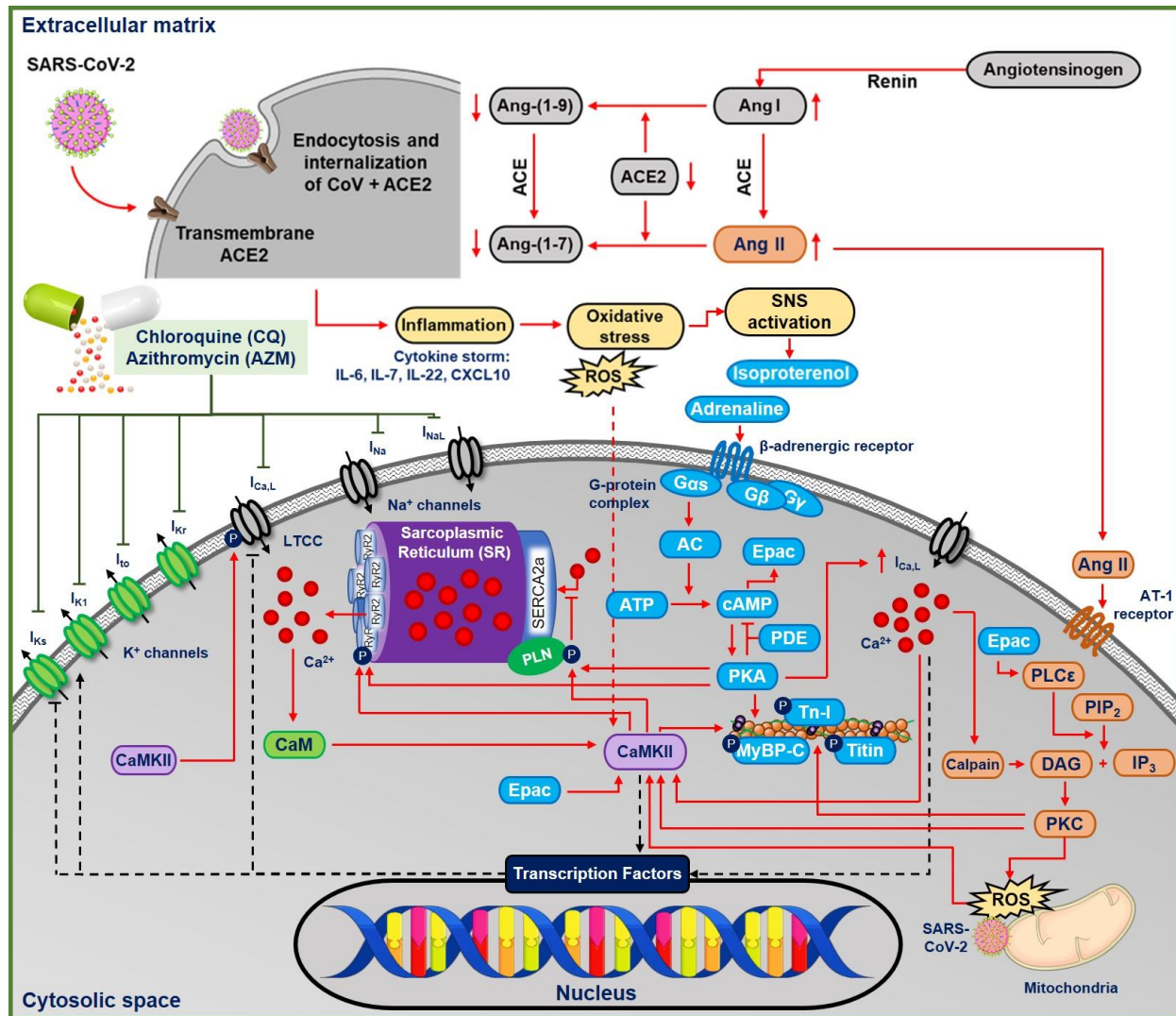


Figure 1. The multifactorial effects of COVID-19 in the ventricular cardiomyocyte and the ionic targets of chloroquine and azithromycin. The SARS-CoV-2 virus leads to the endocytosis and internalizations of the transmembrane ACE2 receptors, preventing the conversion of angiotensin I and II into their metabolites. Thus, angiotensin II binds to the AT-II receptor, initiating PKC-dependent pathways, which may further activate CaMKII-dependent signaling cascades. In COVID-19, the systemic inflammation and cytokine storm can also increase oxidative stress, leading to ROS-mediated CaMKII activation. CQ and AZM alter action potential properties through inhibition of multiple cardiac ion channels (I_{Na} , I_{NaL} , I_{Kr} , I_{Ks} , I_{K1} , I_{to} , $I_{Ca,L}$). (AC = adenylyl cyclase; ACE = angiotensin converting enzyme; Ang II = angiotensin II; ATP = adenosine triphosphate; CaM = calmodulin; CaMKII = calmodulin-dependent protein kinase II; cAMP = cyclic adenosine monophosphate; DAG = diacyl glycerol; IL = interleukin; IP3 = inositol triphosphate; PDE = phosphodiesterase; PIP₂ = phosphatidylinositol biphosphate; PKA = protein kinase A; PKC = protein kinase C; PLC = phospholipase C; ROS = reactive oxygen species; Tn-I = troponin-I)

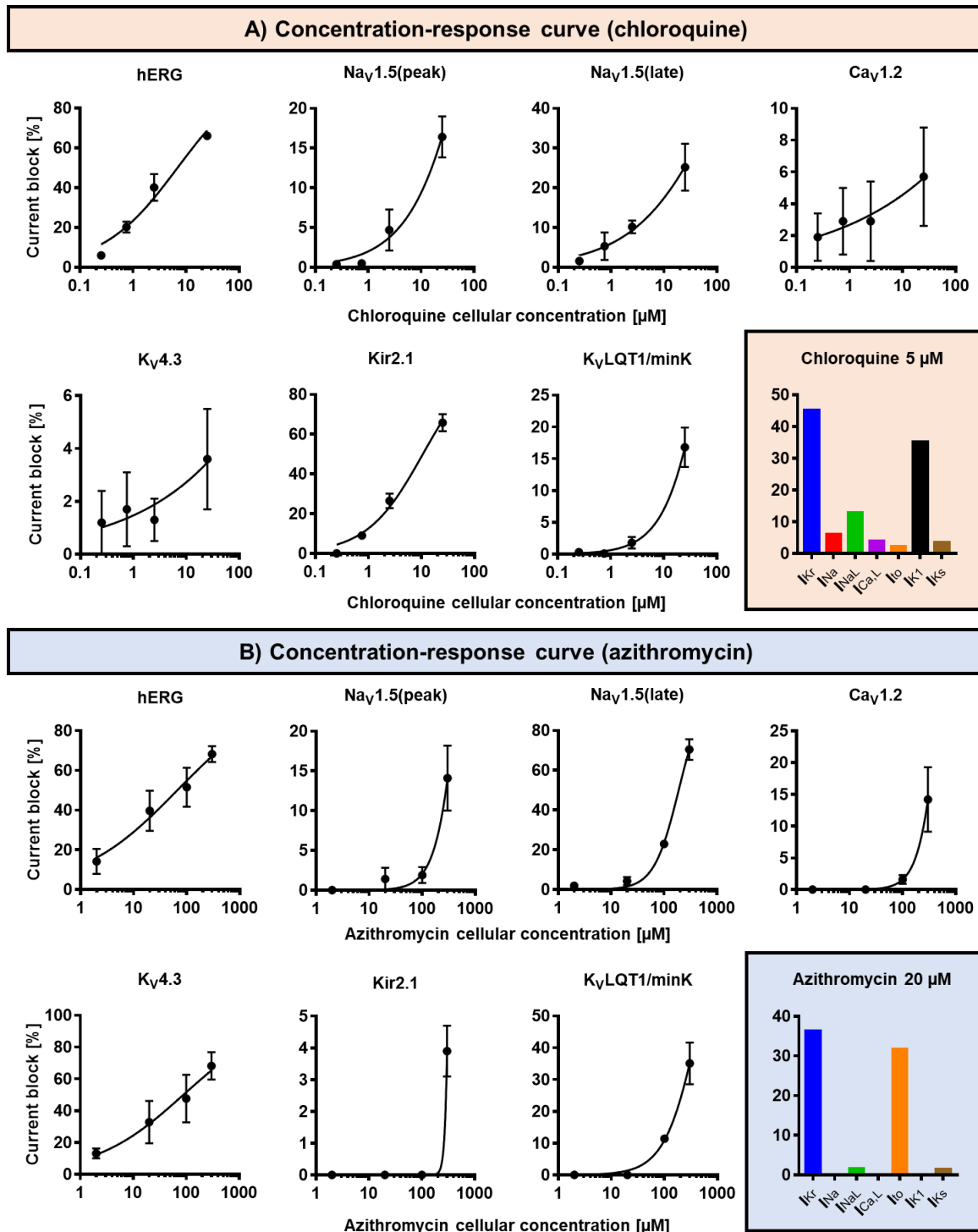


Figure 2. The concentration-dependent effects of chloroquine and azithromycin on cardiac ion channels. A) chloroquine mainly blocks I_{Kr} and I_{K1} , with minor effects on I_{Na} , I_{NaL} , I_{to} , $I_{Ca,L}$ and I_{Ks} . **B)** azithromycin mainly blocks I_{Kr} and I_{to} , with minimal effects on I_{Na} , I_{NaL} , $I_{Ca,L}$, I_{K1} and I_{Ks} . The experimental data (black symbols) were obtained from previous experiments (11) and were fitted using Hill equations in the model (black lines). Bar charts show percentage inhibition of different ion channels using the clinically relevant concentrations employed in subsequent simulations.

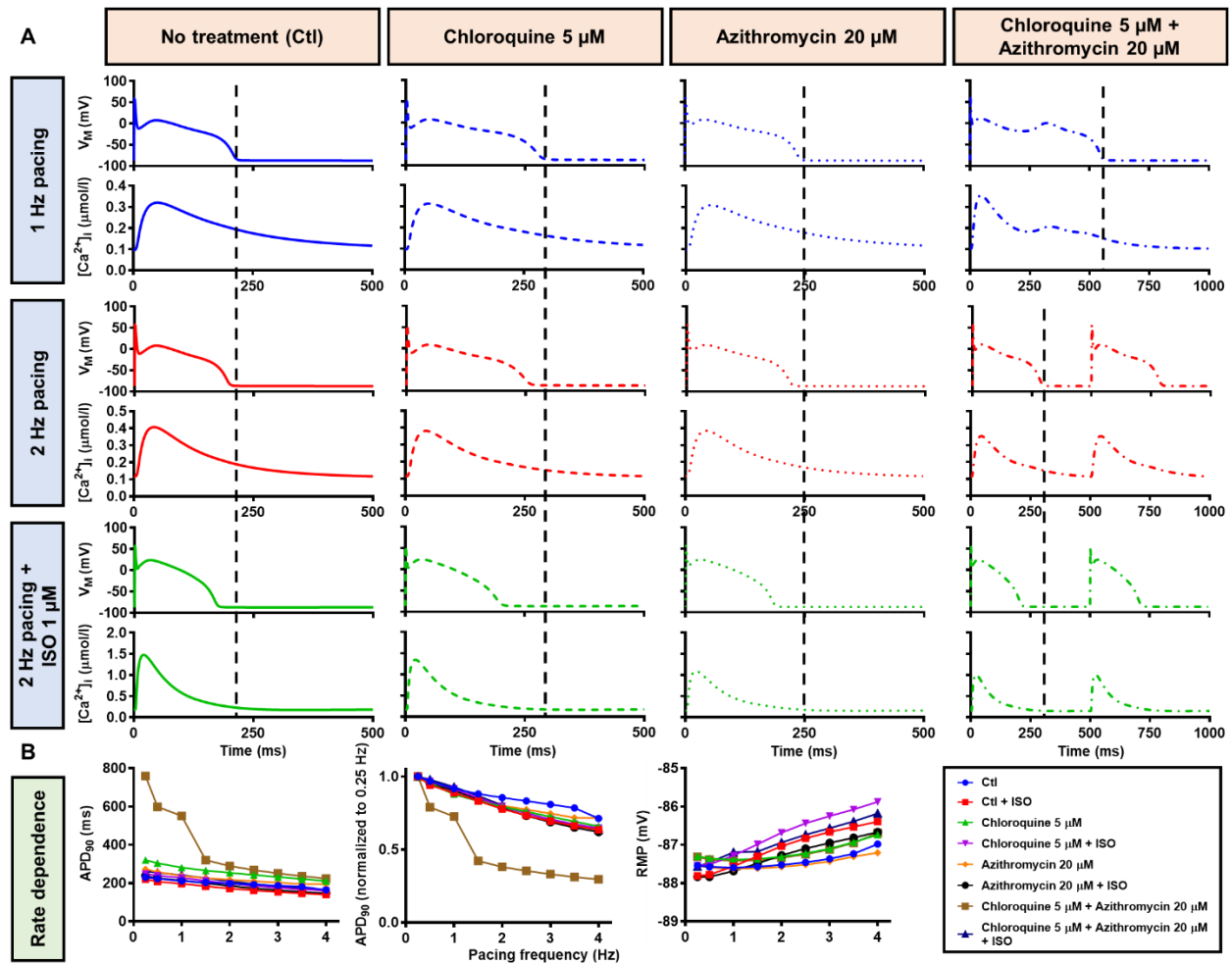


Figure 3. The effects of chloroquine and azithromycin on AP properties. A) The AP and Ca^{2+} transient of non-treated, chloroquine 5 μ M, azithromycin 20 μ M and combined groups. The dashed vertical lines indicate the end of AP in 1 Hz pacing models to provide a clearer depiction of the effects of increasing pacing rate and ISO on APD. **B)** APD and RMP for different pacing rates in the four groups with and without simulated beta-adrenergic stimulation. (AP = action potential; APD = action potential duration; Ctl = control; ISO = isoproterenol; RMP = resting membrane potential)

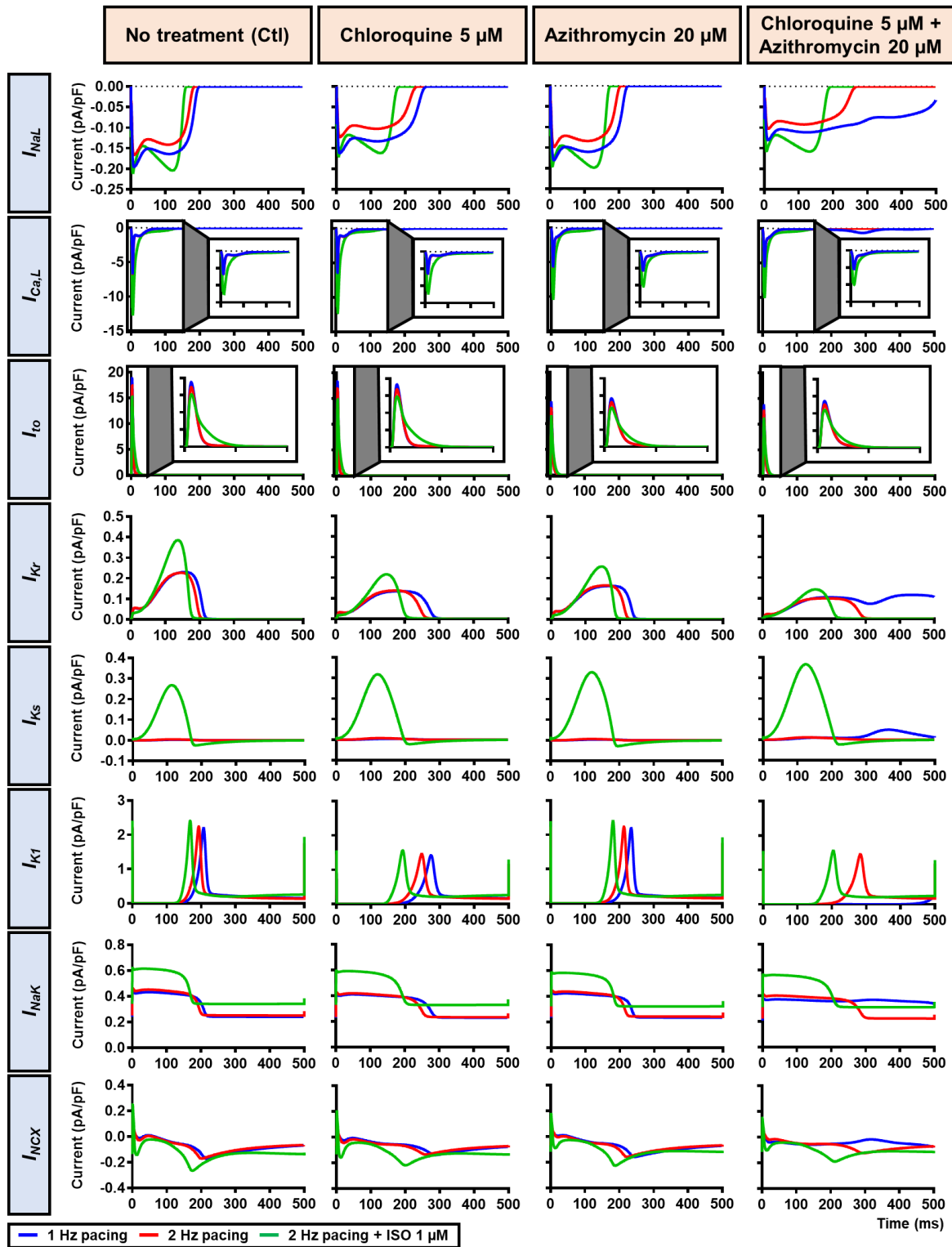


Figure 4. The effects of beta-adrenergic response on cardiac ion channels. The effects were assessed in 4 groups: non-treated, chloroquine, azithromycin and combined groups. The blue lines represent the ionic currents during 1 Hz pacing, the red lines represent the ionic currents during 2 Hz pacing and the green lines represent the currents during 2 Hz pacing with ISO 1 μ M. The L-type Ca^{2+} current ($I_{\text{Ca,L}}$) and transient-outward K^{+} current (I_{to}) are shown at an expanded scale in the insets.

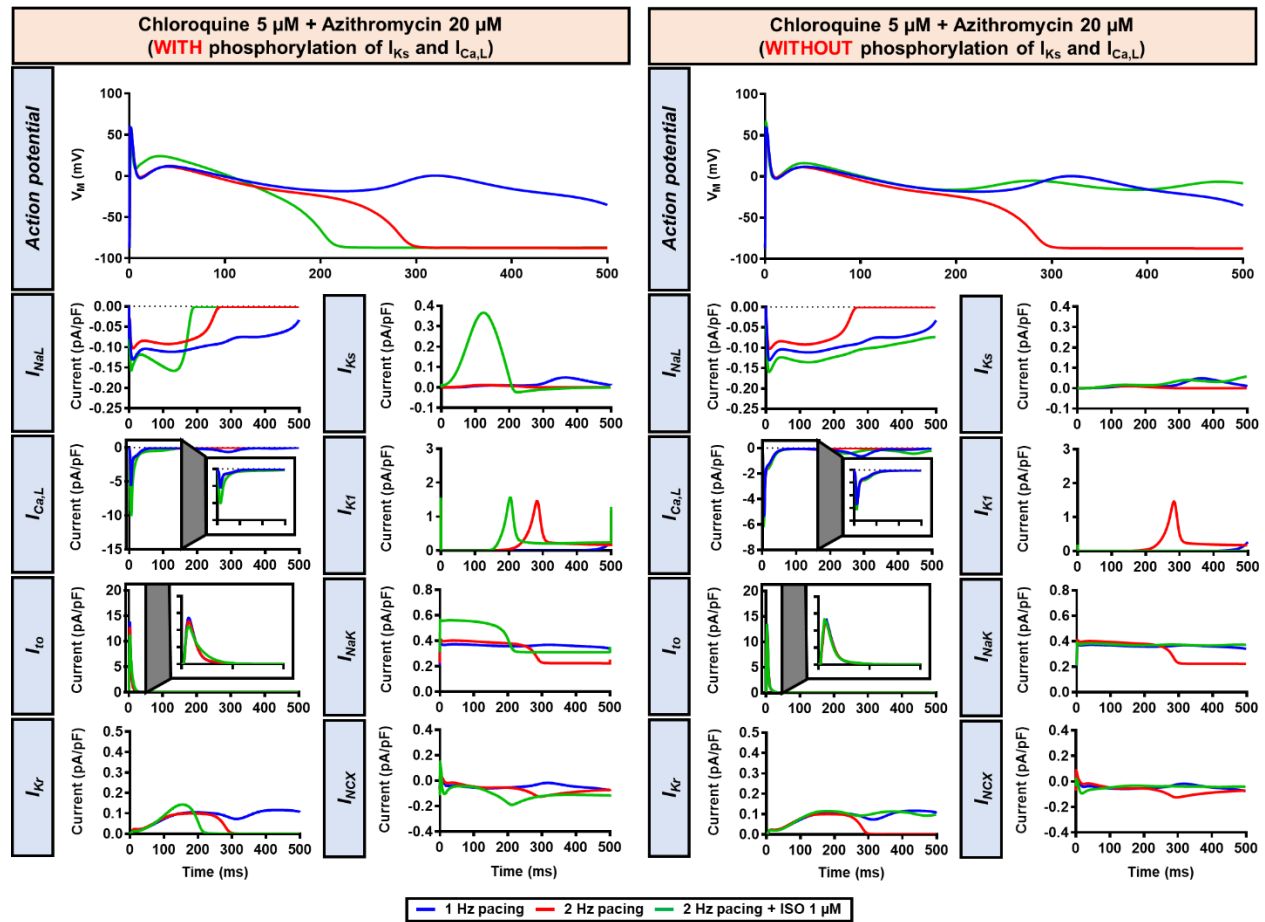


Figure 5. The role of I_{Ks} and $I_{Ca,L}$ phosphorylation on the action potential in the presence of chloroquine and azithromycin. The left panel showed the effect of CQ 5 μM in combination with AZM 20 μM in the presence of ISO-induced I_{Ks} and $I_{Ca,L}$ phosphorylation. The right panel showed the effect of CQ 5 μM in combination with AZM 20 μM in the absence of ISO-induced I_{Ks} and $I_{Ca,L}$ phosphorylation.

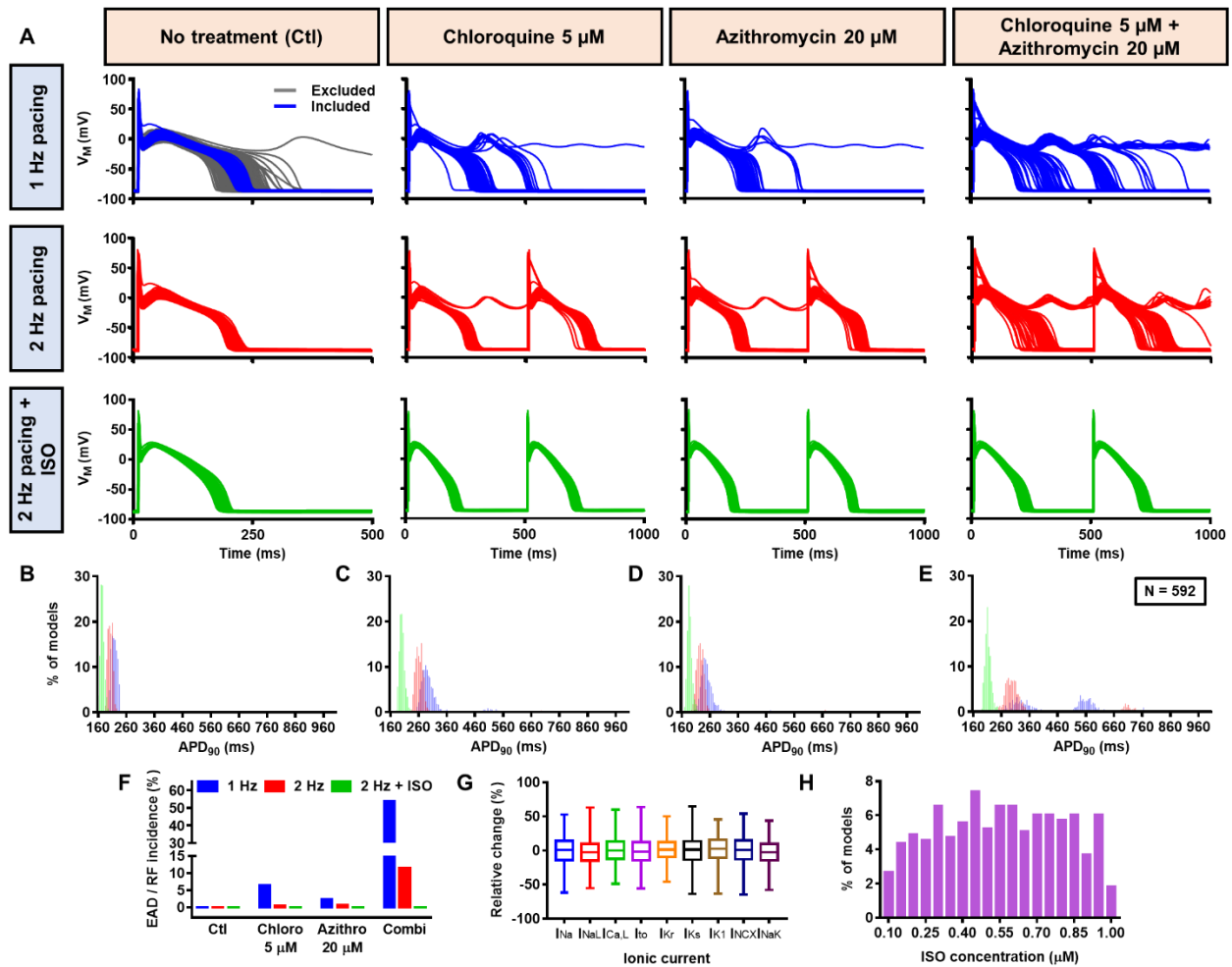


Figure 6. The cellular effects of chloroquine and azithromycin in the population of 1000 canine ventricular epicardial myocyte models. A) The APs of 592 models included in the study, with the 408 excluded non-physiological APs shown as grey lines. **B-E)** The frequency distribution of APD in non-treated, chloroquine, azithromycin and combined groups. **F)** The incidence of EAD/RF observed in the population-based study (in percentage of models). **G)** Boxplot showing the distribution of relative changes on ionic currents to accommodate the interindividual variability. **H)** The frequency distribution of random ISO concentration employed in the study.